Machine Vision and Applications (2006) 17:327–336
DOI 10.1007/s00138-006-0038-y

ORIGINAL PAPER

Tool condition classification using Hidden Markov Model based on fractal analysis of machined surface textures

A. A. Kassim · Zhu Mian · M. A. Mannan

Received: 27 December 2005 / Accepted: 5 June 2006 / Published online: 22 July 2006

Abstract The texture of a machined surface generated by a cutting tool, with geometrically well-defined cutting edges, carries essential information regarding the extent of tool wear. There is a strong relationship between the degree of wear of the cutting tool and the geometry imparted by the tool on to the workpiece surface. The monitoring of a tool's condition in production environments can easily be accomplished by analyzing the surface texture and how it is altered by a cutting edge experiencing progressive wear and micro-fractures. This paper discusses our work which involves fractal analysis of the texture of surfaces that have been subjected to machining operations. Two characteristics of the texture, high directionality and self-affinity, are dealt with by extracting the fractal features from images of surfaces machined with tools with different levels of tool wear. The Hidden Markov Model is used to classify the various states of tool wear. In this paper, we show that fractal features are closely related to tool condition and HMM-based analysis provides reliable means of tool condition prediction.

Keywords Tool wear monitoring · End-milling · Surface texture analysis · Fractal analysis · Hidden Markov Model

A. A. Kassim (✉) · Z. Mian
Department of Electrical and Computer Engineering,
National University of Singapore,
Singapore, Singapore
e-mail: ashraf@nus.edu.sg

M. A. Mannan
Department of Mechanical Engineering,
National University of Singapore,
Singapore, Singapore

1 Introduction

In machining operations, cutting tools are discarded once their expected lifespan is reached. However, the usefulness of these tools very often exceeds the expected lifespan and many tools are discarded even when they can still be used. Conversely, if a machine tool fails before reaching its expected lifespan, it could potentially damage the machine and the material being processed. With real-time tool wear monitoring, it is possible to ascertain the level of tool wear and therefore only change the tools when they reach their maximum useful life. Various techniques have been proposed for tool wear monitoring and an extensive review, including those involving acoustic emission, tool temperature, cutting forces, and vibration signatures, is presented in [1]. However, due to the complexity of the tool wear process, reliable online tool wear monitoring remains a challenge. In this paper, we propose a new surface texture characterization approach to tool wear monitoring.

During machining operations, the quality of the machined surface changes as the tool wears. There is a strong relationship between the degree of wear of the cutting tool and the geometry imparted by the tool on to the workpiece surface [2]. Since the tool operates directly on the workpiece, the machined surface carries valuable information about the machining process including tool wear, built-up edge, and vibrations, which in turn provides reliable and detectable information to categorize the condition of the cutting tool. Random process analysis techniques are applied to characterize the machined surfaces in [3]. In a previous work [2, 4], the degrees of tool wear during *turning* operations were successfully ascertained by texture analysis of images of machined surfaces using *column projection* and *run*

length statistics. In this paper, we focus on analysis of the texture of *end-milled* surfaces.

Figure 1 shows images of end-milled surfaces produced by a cutting tool when it is *sharp* (new), *semi-dull* (flank wear of 0.3 mm), and *dull* (flank wear of 0.5 mm). Figure 2 shows the images of turned surfaces for different stages of tool wear. Clearly, the texture of end-milled surfaces is quite different from that of turned surfaces. The surface texture produced by the turning operation is characterized by equally displaced grooves (Fig. 2a) and as the tool wears, wear particles become more evident as illustrated by Figs. 2b,c. On the other hand, surface textures produced by end-milling operations are irregular and more complex. The vision-based methods in [2, 4] which have been successfully used for analyzing surfaces produced by turning operations cannot be used for analyzing textures produced by end-milling operations because the regular features required by these methods are simply not evident in the surfaces produced by end-milling operations.

Fractal analysis is a relatively new but powerful tool for texture analysis. In this paper, we investigate the use of fractal analysis to characterize surfaces milled with tools having experienced different levels of tool wear and Hidden Markov Models (HMM) to classify the various degrees of tool wear. While HMM-based methods have been used extensively, this is believed to be the first work to use fractals with HMMs to analyze changes in texture images.

The paper is organized as follows. Fractal analysis is discussed in Sect. 2 and a brief introduction to the HMM is provided in Sect. 3. The experimental setup is presented in Sect. 4. An explanation of how the fractal features are obtained from textures of end-milled surfaces and their use with the HMM is provided in Sect. 5. We present and discuss the experimental results in Sect. 6, and provide our conclusions in Sect. 7. Some nomenclatures used in this paper are summarized in Table 1.

Table 1 Nomenclature List

Vb_{max}	The maximum flank wear of the tool
λ	Notation of Hidden Markov Model
A	State transition probability matrix
B	Observation probability distribution
π	Initial state probability distribution
G_m	Gaussian distribution
$P(x)$	Probability of event x
$p(x)$	Probability density function of x
$E(x)$	Expectation of x
FD	Fractal dimension
$I(x)$	Image intensity profile

2 Fractal analysis

Fractals have been successfully applied in analyzing various chaotic phenomena [5] because many natural objects demonstrate self-similarity over a range of scales. *Fractal Dimension* (FD) is the parameter that measures the extent of self-similarity. The realization that the FD shows close correspondence to human perception of texture [6] has motivated research into possible applications of fractal analysis in image processing and computer vision. The FD has been used for image segmentation [6], finger print identification [7], and characterizing surface topology [8].

2.1 Estimating the fractal dimension

Many methods have been proposed to estimate the FD [5]. These methods vary in computational efficiency, numeric precision, and estimation boundary. Thus, FDs estimated by different methods may carry different information about fractal objects. We used two FD estimation methods in our work.

2.1.1 Method 1

The one-dimensional (1D) image profile can be approximated by fractal Brownian motion function [7]. The *image profile* is the set of gray level values along an arbitrary line across the image. Figure 3 shows an example of image profiles, which is obtained along the vertical line in the middle of Fig. 1a.

A fractal Brownian motion function $I(x)$ has the property that the mean value of its absolute differences, $E(|\Delta I(x)|)$, is proportional to $|\Delta x|^H$, where H is called the *Hurst coefficient*. Taking the logarithm, we obtain

$$\log E(|\Delta I(x)|) = H \log |\Delta x| + \text{constant} \quad (1)$$

In this paper, $I(x)$ is represented by the image intensity value, and x is the distance along the profile as shown in Fig. 3. Thus, H can be estimated by applying least square regression for different values of Δx and therefore $E|\Delta I(x)|.E|\Delta I(x)|$ is computed by taking the average of all $|\Delta I(x)|$ determined by Δx. The FD of the fractal Brownian motion function is simply $2–H$ [7].

2.1.2 Method 2

The box counting (BC) algorithm [5] can be used to compute the FD of 2D images of machined surfaces. As shown in Fig. 4, the machined surface viewed as a 3D surface is divided into cubic cells or boxes, each side of length r. The number of cells, $N(r)$, through which any part of the surface passes through, is proportional to

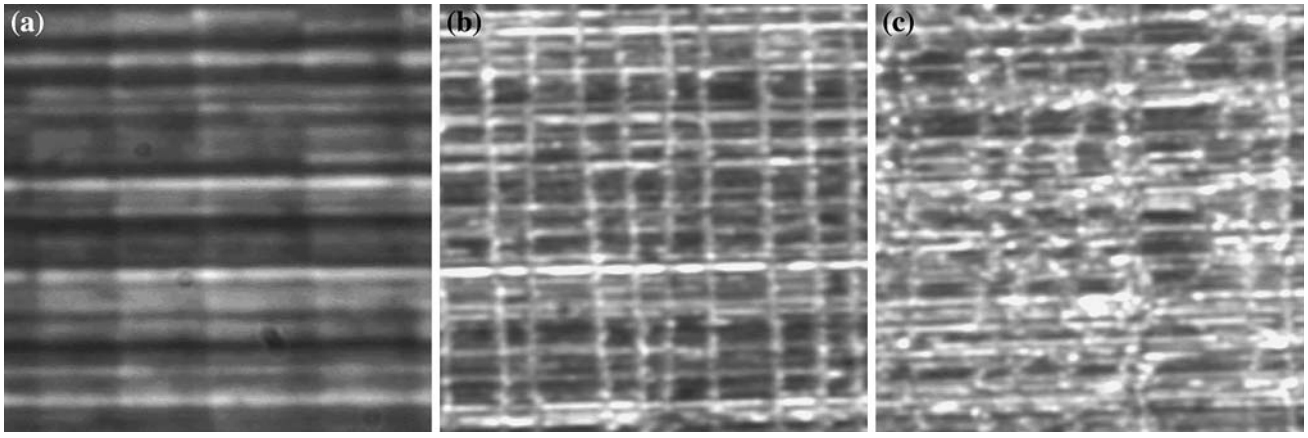

Fig. 1 Textures of machined surfaces produced by end-milling operations when the tool is **a** sharp, **b** semi-dull, and **c** dull (Vb_{max} = 0.5 mm). The size of the image is 1.1 mm×1.1 mm

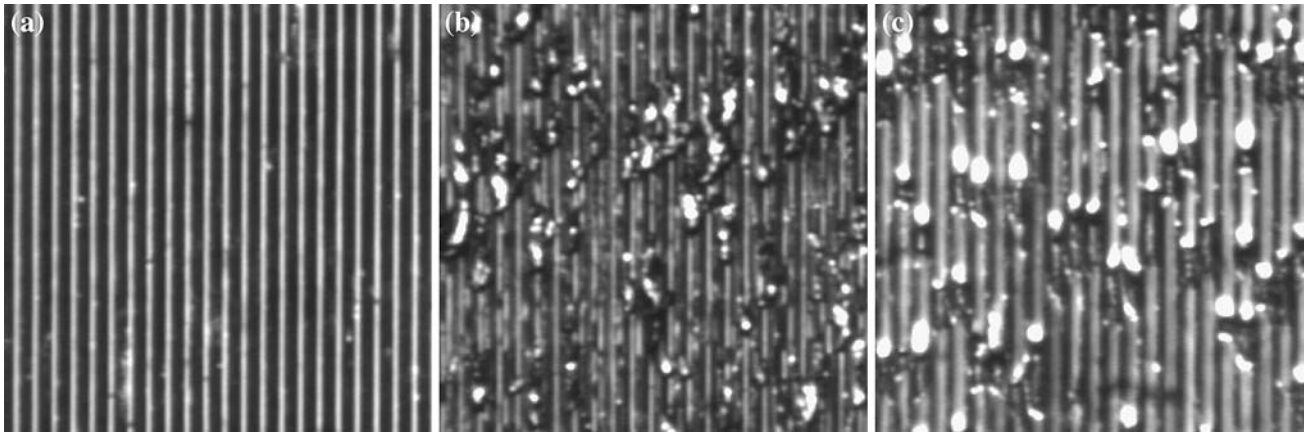

Fig. 2 Textures of machined surfaces produced by the turning operation when the tool is **a** sharp, **b** semi-dull, and **c** dull (Vb_{max} = 1.0 mm). The size of the image is 1.1 mm×1.1 mm

$r^{-\mathrm{FD}}$, where FD is the BC dimension of the image. By choosing different side lengths r, FD can be estimated by using linear regression as in Method 1.

In general, the FD can be computed by measuring certain metric property M over different scales ϵ [7]. In Methods 1 and 2, the mean difference $E|\Delta I(x)|$ and the number of visited cells $N(r)$ are metric properties, while Δx and r are the respective scale variables. The FD is estimated as follows:

- Compute the metric property $M(\epsilon)$ for different scales ϵ.
- Apply least square regression to the plot of $\log(M)$ versus $\log(\epsilon)$.
- Derive FD from the slope.

2.2 Fractal analysis of end-milled surfaces

Fractal features are chosen in this work because they should be able to better represent the irregular textures of end-milled surfaces than other types of features that rely on the regularity of textures. Fractal analysis of end-milled surface textures involves computing the FD of both image profiles and images themselves, which are self-affine and not self-similar. The FD of self-similar curves and surfaces satisfy

$$D_{\mathrm{T}} < \mathrm{FD} < D_{\mathrm{T}} + 1 \tag{2}$$

where D_{T} is the topological dimension, and $D_{\mathrm{T}} = 1$ for 1D curves and $D_{\mathrm{T}} = 2$ for 2D images. Equation (2) is a prerequisite condition of a fractal set in a strict mathematical sense, but the estimated FD of self-affine objects may not satisfy this condition. For this reason, the slope of log–log plot is used as a fractal feature in this work.

The texture of end-milled surfaces is *anisotropic*. The issue of characterization of anisotropic surfaces has been well studied. In [8], the 2D Fourier transform is applied to anisotropic surfaces and the slope of the log (magnitude^2) versus log (frequency) plot is evaluated as

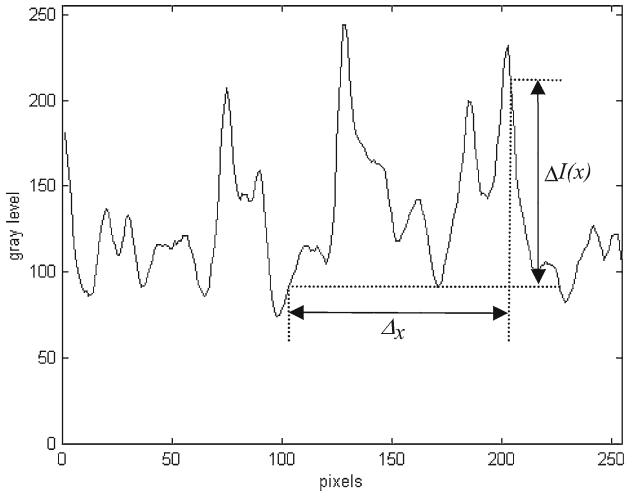

Fig. 3 Profile of the end-milled surface image

a function of direction by dividing the frequency domain into several pie-shape regions similar to Fig. 5. Li et al. [9] proposed a new parameter to measure the anisotropy based on profile spectral moments and surface spectral moments of machined surfaces. Thomas et al. [10] used the structure function (related to the autocovariance function) of machined surfaces, to estimate the FD and *topothesy*, and studied their relationship to anisotropy. Topothesy, which is defined in the Weierstrass–Mandelbrot function [9], is derived from the intercept of the log–log plot of power spectrum versus frequency, which is more sensitive to anisotropy than the FD [8].

In our work, the anisotropic nature of end-milled surfaces is addressed by analyzing fractal features for the image profiles along different directions. The *slopes* and *intercepts* of log–log plots are directly used as fractal features that account for *roughness* and the *directionality of the texture*, respectively. Figure 5 shows the slope and intercept of profiles as a function of angular direction. The image profiles are extracted from Fig. 1a. It is clear that the intercept varies greatly as the direction of profile changes.

3 Hidden Markov Model

The main objective in tool wear monitoring is to detect tool wear states from sensory signals. However, the sensory signals are also affected by many factors including the operational mode of the machine (including cutting parameters, use of coolant, etc.), type of workpiece material, composition of the tool, and noise from various sources. Neural network techniques [2] have been successfully used to overcome these effects.

Unlike the neural networks approach, the HMM uses Markov chains to model dynamic processes. The HMM is a stochastic model that describes piecewise stationary random processes and had been originally used for speech recognition [11]. Recent work has focused on the use of the HMM to classify and detect tool wear states. The HMM has been used to detect tool wear stages in drilling operations [12]. In [13], the vibration signals of end-milling operations are analyzed in different time scales and the HMM is used to categorize the states of tool wear from these signals.

Tools experience several stages of tool wear before they are worn out [12]. In our work, we explore the use of the HMM approach to reveal the inherent structure of the tool wear process. The aim is to investigate whether different tool wear stages, such as *sharp*, *slight-worn*, *semi-worn*, and *worn-out*, can be effectively modeled by the discrete states of a HMM.

The basic elements of a four-state left–right HMM model are exemplified in Fig. 6. N denotes the number of states in the system and the observation sequence $O = O_1O_2O_3 \cdots O_N$ is the only part accessible to the outside world. Some important characteristics about HMM model are listed below:

- At any given time t, the system will stay in one of the discrete states $q_t = S_i$ where $1 \leq i \leq N$ and q_t is the current system state.
- The state transition from S_i to S_j can be made at next event $t+1$ with probability $a_{ij} = P[q_{t+1} = S_j | q_t = S_i]$. A basic assumption of Markov chains is that the probability of a system being in a state at time $t+1$ depends only on the current state at time t and is independent of all previous states.
- The observations are random variables that are either discrete $\{v_1, v_2, \ldots, v_M\}$ or continuous, v, with probability distribution functions $P(v_j|q_t = S_i)$ and $p(v|q_t = S_i)$, respectively. For continuous observations, $p(v|q_t = S_i)$ is usually modeled as the weighted sum of Gaussian distributions, i.e., $p(v|q_t = S_i) = \sum_{m=1}^{M} c_{im} G_m(\mu_{im}, U_{im})$, where G_m is the Gaussian distribution with mean μ_{im} and variance U_{im}.

The HMM is specified by the *state transition probability matrix* $A = \{a_{ij}\}$, the *observation probability distribution* $B = \{b_{ij}\}$ or $B = \{c_{ij}, \mu_{ij}, U_{ij}\}$, and the *initial state probability distribution* $\pi = \{\pi_i\}$, where π_i is the probability of being in state S_i at the beginning of the observation sequence. Thus, the HMM is often denoted as $\lambda(A, B, \pi)$.

The basic issues of HMM are the *evaluation* of the probability of observation sequence $P(O|\lambda)$ given the observation sequence $O = O_1O_2 \cdots O_N$ and the model

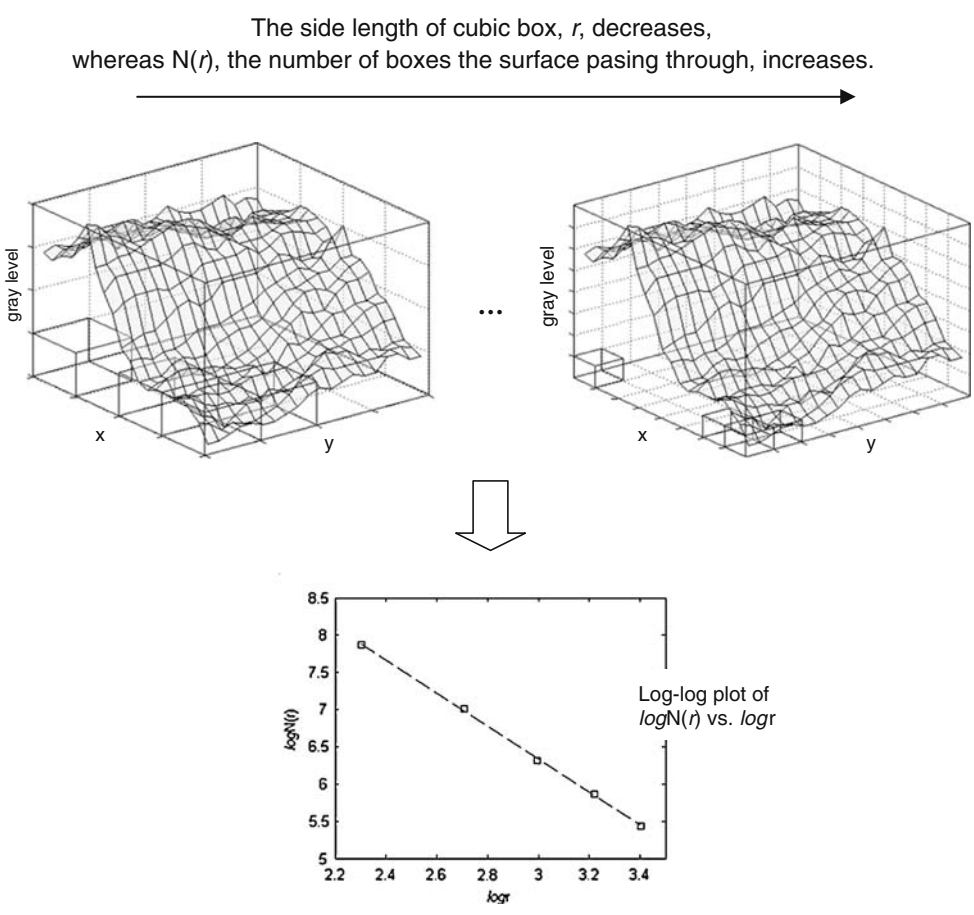

Fig. 4 Box counting method

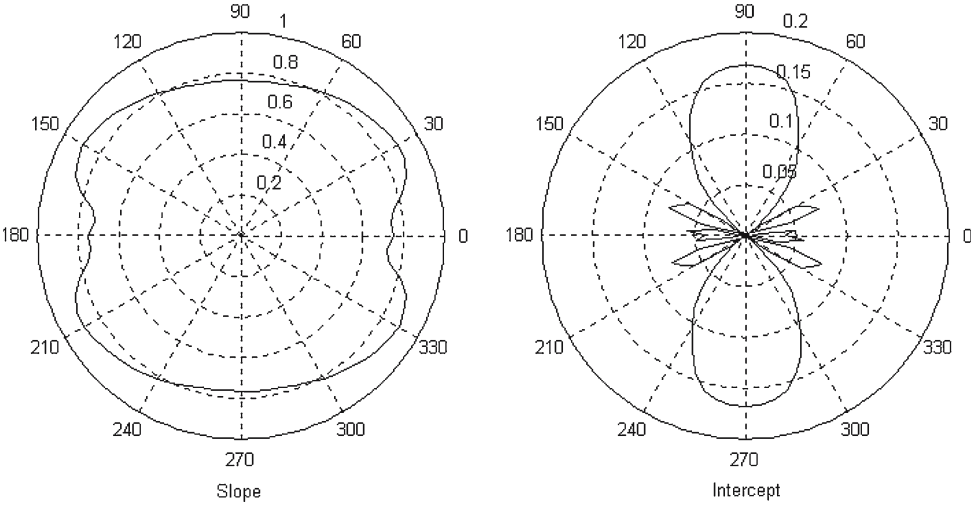

Fig. 5 Slope and intercept of profiles along different angular directions

$\lambda = (A, B, \pi)$; the *decoding* of the most likely state sequence $Q = q_1 q_2, \ldots, q_t$, given the observation sequence $O = O_1 O_2 \cdots O_N$ and the model $\lambda = (A, B, \pi)$; and the *estimation* of the model $\lambda = (A, B, \pi)$ to maximize $P(O|\lambda)$ given the observation sequence $O = O_1 O_2 \cdots O_N$. Standard algorithms for resolving these issues include the forward-backward procedure, Veterbi algorithm, and Baum–Welch method [11].

In our work, we investigate two problems:

1. *Detection problem:* determining the most likely state q_t at time t, given a HMM model and observation sequence.
2. *Prediction problem:* determining the probability that the next state will be the tool-worn-out state.

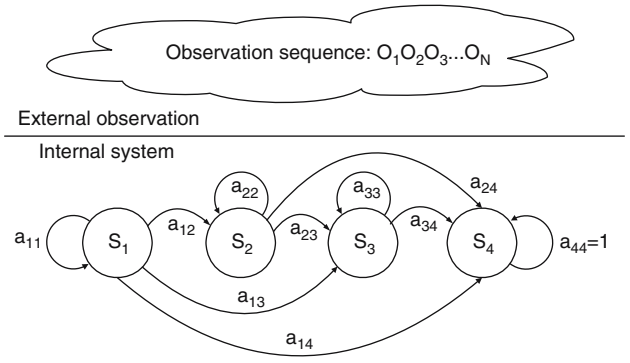

Fig. 6 Left–right HMM

These two problems are of practical importance in tool wear monitoring. Given the observation sequence of fractal features, solving the detection problem will give the current tool wear state at certain time t, and the outcome of prediction problem is the probability of the event "tool is worn out at next time event".

For the detection problem, we use the variable $\gamma_t(j) = P[q_t = S_j|O, \lambda]$ [11], which is the probability of being in state S_j, given the observation sequence O and the model λ. $\gamma_t(j)$ can be expressed as

$$\gamma_t(j) = \frac{\alpha_t(j)\beta_t(j)}{P(O|\lambda)} = \frac{\alpha_t(j)\beta_t(j)}{\sum_{i=1}^{N} \alpha_t(i)\beta_t(i)} \tag{3}$$

where α_t and β_t are forward and backward variables in the forward–backward procedure [11]. Using $\gamma_t(j)$, the best estimate of q_t is

$$q_t = \arg\max_{1 \le j \le N}[\gamma_t(j)] \quad 1 \le t \le \mathrm{T} \tag{4}$$

The prediction problem can be solved by

$$P[q_{t+1} = S_N|\lambda] = \sum_{i=1}^{N} P[q_t = S_i|\lambda]a_{iN} = \sum_{i=1}^{N} \gamma_t(i)a_{iN} \tag{5}$$

where S_N is the final state of left–right HMM model and is defined as the "tool-worn-out" state.

4 Experimental setup

In our experiments, aluminum workpieces are milled without using coolants by a 16 mm diameter high-speed steel end mill at a rotational speed of 2,000 rpm, radial depth of cut of 3 mm, axial depth of cut of 16 mm, and feed rate of 180 mm/min.

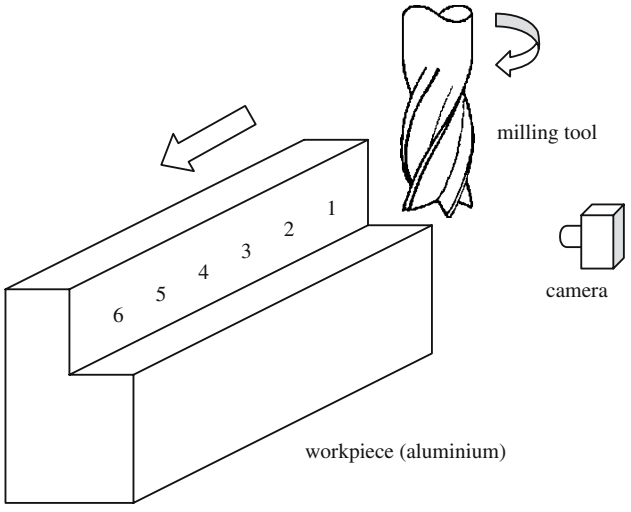

Fig. 7 Experimental setup

After each *pass* of the milling process, the flank wear of the milling tool is measured and when the flank wear shows an increase of 0.1 mm, images of the milled aluminum workpiece are taken at six different locations. This process is repeated until the flank wear reaches 0.5 mm. Figure 7 shows the experimental setup and the positions (numbered 1, 2, 3, 4, 5, 6) at which the images are taken. The PC-based image capturing system uses a CCD camera with appropriate magnification and illumination. The images of the surfaces were captured as 256 gray level images and are numbered sequentially. Images #1 to #6 are taken during the first pass when the flank wear of the milling tool is almost negligible, images #7 to #12 are taken after the flank wear reaches about 0.1 mm and so on until a flank wear of 0.5 mm is achieved. Image #19, for example, is taken (at the same positions as images #1, #7, and #13) after the tool flank wear reaches about 0.3 mm. Therefore, the image number is an index of both time and the state of tool wear. We obtained 15 image sequences of 36 images each that show the changes in the machined surface texture as tool flank wear progresses from 0.1 to 0.5 mm.

5 Using the fractal features with the Hidden Markov Model

The fractal features extracted from each surface image form a sequence of observations. A left–right HMM model is used to detect the inherent tool wear states

behind the observations. We discuss below how the fractal features are obtained and the training of HMM is discussed in Sect. 5.1.

Fractal feature extraction is carried out on 256 × 256 images of the machined surface. The fractal features are obtained using Method 1 (image profiles) and Method 2 (BC). Method 1, which deals with the anisotropy of the surface images, estimates the fractal features from image profiles along the 0°, 30°, 60°, 90°, 120°, and 150° directions. The fractal features are simply the slopes and intercepts of the log–log plots of log $\mathrm{E}(|\Delta I(x)|)$ versus $\log|\Delta x|$. Because the image is digitized in both position and gray levels, it can only demonstrate fractal property over a certain range. Therefore, in Method 1, the distance Δx is set to the range of $2 \leq \Delta x \leq 8$ pixels. In Method 2, the range of size r is set to $10 \leq r \leq 30$ pixels.

A total of 14 fractal features are available where 12 features are extracted from image profiles along six different directions and the remaining two features are the slope and intercept of the log–log plot using Method 2. Table 2 shows the extracted values corresponding to the flank tool wear using Method 1 and Method 2 for a particular test run. It is evident that except for the slope corresponding to the 0° profile, most slope and intercept values change proportionally or inverse proportionally to the tool condition and the rate of change varies with the anisotropy.

We formulated a 13-element feature vector which includes all slope and intercept values except for the slope of the 0° profile. As the texture of the machined surface is highly anisotropic, it is necessary to use the information in all 13 feature elements which essentially represent the absence/presence of features in the different directions. The 13-element feature vector forms the multidimensional observation sequence that is used to train the HMM model.

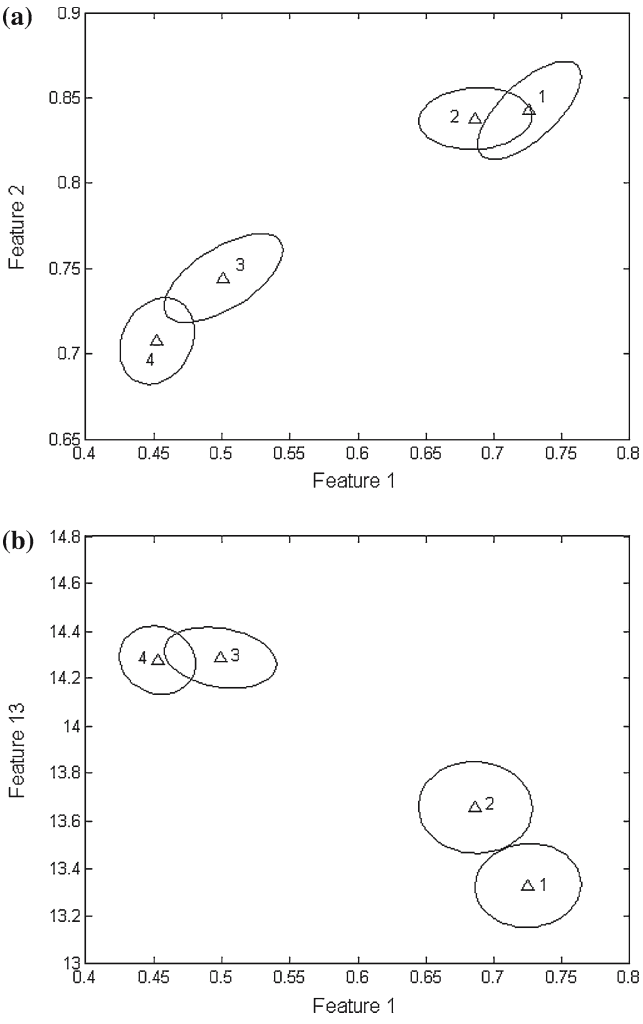

Fig. 8 Training result in **a** feature1–feature2 space and **b** feature1–feature13 space

5.1 HMM training

We obtained 15 image sequences (of 36 images each) that represent the changes in the machined surface texture as tool flank wear progresses from 0.1 to 0.5 mm. Ten sequences are used as training images while the remaining five sequences (180 images) are used as test images. Fractal features extracted from these image sequences are used as the observation sequences of HMM model.

A left–right HMM is used because it effectively models a one-way process such as the tool wear process [12]. The observation is modeled as a unimodal multidimensional Gaussian distribution. From our experiments, it was found that using four states produced desirable results. The Baum–Welch method is applied to train the HMM, i.e., estimate the parameters in $\lambda = (A, B, \pi)$.

Figure 8 shows the four HMM states detected in the training image sequences. The progress through the states highlights the progress of tool wear, i.e., the tool is sharp in State 1, semi-dull in State 2 and 3, and worn out in State 4. The training result in 2D feature space is shown in Fig. 8. The selection of the two features is arbitrary as similar plots are obtained when any two feature elements are used. In Fig. 8, features 1 and 2 are slopes corresponding to the 90° and 30° profiles, respectively, while feature 13 is the intercept obtained from Method 2. The overlapping of states in Fig. 9 would be reduced or avoided as more features are used (i.e., in a multidimensional feature space).

Table 2 Typical fractal feature values versus flank tool wear

Features		Flank tool wear					
		0 mm	0.1 mm	0.2 mm	0.3 mm	0.4 mm	0.5 mm
Profile direction		Method 1					
0°	Slope	0.6817	0.7324	0.7435	0.7235	0.7153	0.6972
	Intercept	0.0513	0.0457	0.0748	0.1705	0.1912	0.1964
90°	Slope	0.7224	0.6990	0.6946	0.5076	0.4706	0.4550
	Intercept	0.1528	0.1805	0.2026	0.3527	0.3726	0.3902
30°	Slope	0.8426	0.8398	0.8389	0.7530	0.7108	0.7128
	Intercept	−0.0871	−0.0829	−0.0541	0.585	0.0987	0.0905
120°	Slope	0.7746	0.7576	0.7512	0.5893	0.5624	0.5477
	Intercept	0.0854	0.1036	0.1263	0.2624	0.2592	0.2827
60°	Slope	0.7696	0.7569	0.7504	0.5878	0.5605	0.5438
	Intercept	0.0856	0.0975	0.1216	0.2652	0.2622	0.2851
150°	Slope	0.8483	0.8465	0.8450	0.7630	0.7182	0.7270
	Intercept	−0.1019	−0.0855	−0.0577	0.505	0.0861	0.0741
		Method 2					
	Slope	−2.2414	−2.2423	−2.2991	−2.4009	−2.3853	−2.4021
	Intercept	13.3230	13.4133	13.7225	14.3363	14.1778	14.3277

6 Experimental results and discussion

The trained HMM model is applied on the fractal features extracted from the test data set of 180 images to detect and predict the tool wear state. The extracted fractal features form observation sequences and the Veterbi decoding algorithm is applied to detect the state for each test image. All four states are clearly evident in Fig. 9 which shows the classification results of all 180 test images. Some states overlap in the two-feature space but they can be separated by using more features. The evolution of tool wear illustrated in Fig. 10 for the various test sequences is obtained using the state detection algorithm. The state of a particular image provides an estimate about the tool wear. In Fig. 10, the actual flank wear is plotted as straight lines and the state is represented by circles (one for each of the 180 test images). It can be seen that as the flank wear increases from 0 to 0.5 mm, the tool wear state changes accordingly. It starts from sharp tool (State 1), evolves through intermediates states (State 2 and State 3), and finally reaches the worn state (State 4).

The tool wear process is essentially a state transition process. Tool wear starts from the sharp state, goes through several intermediate states, and finally reaches the dull state. These state transitions are often hard to capture due to the complexity of the tool tear mechanism and noise. Clearly, the results show that features extracted using fractals and the HMM are a very effective means for capturing these transitions. This is more appropriate because in tool condition monitoring the interest is not in the absolute level of the tool wear but

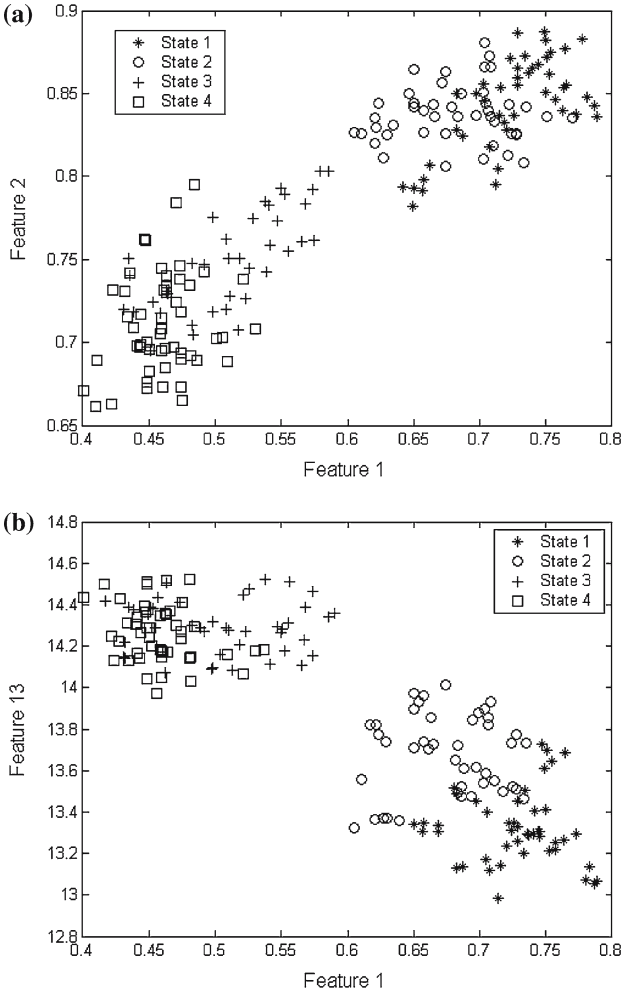

Fig. 9 Classification result for the 180 test images

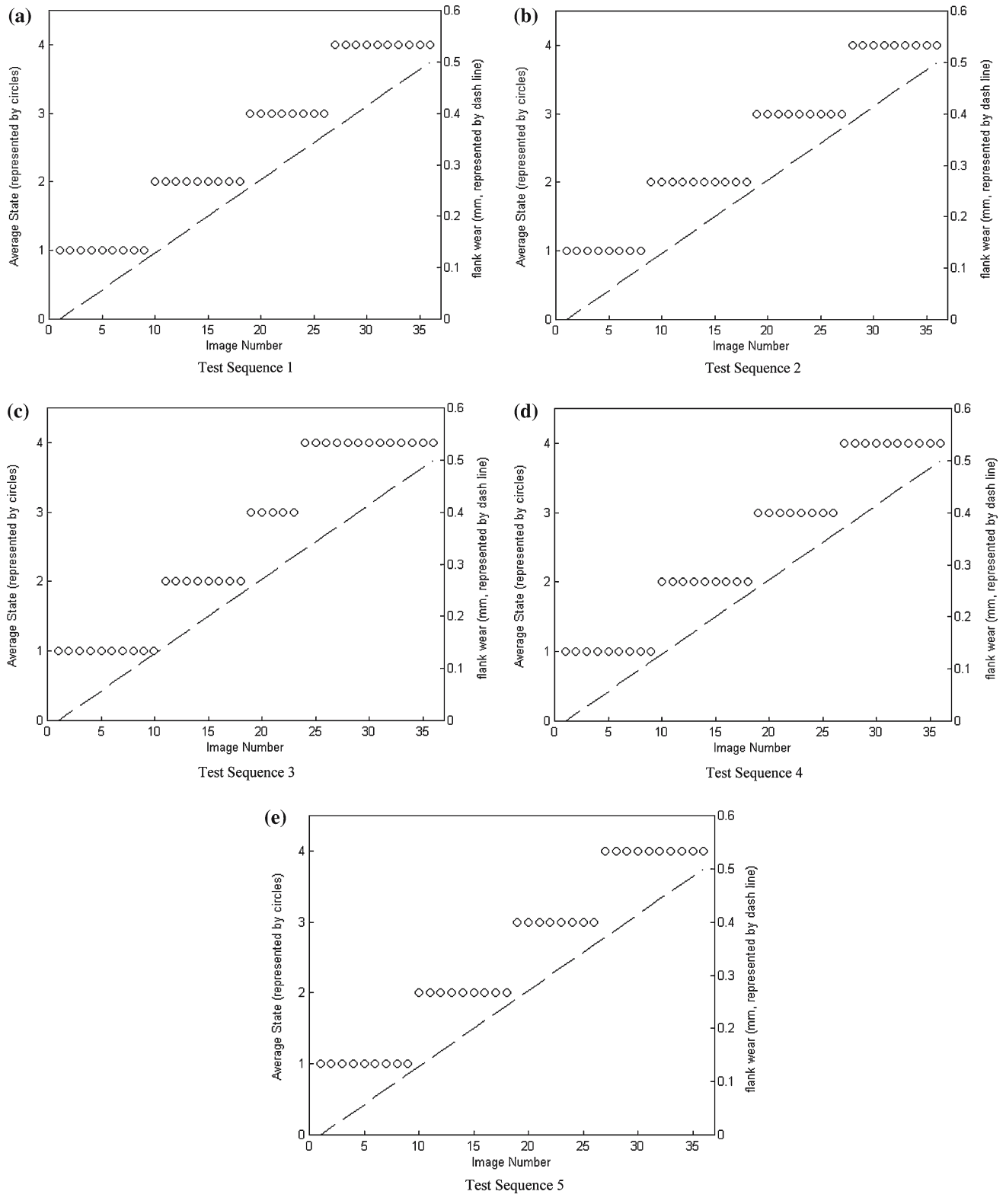

Fig. 10 Estimated states for each of the five test sequences

in the tool condition which can be expressed as sharp, semi-sharp/semi-dull, or dull.

7 Conclusions

In this paper, the fractal characteristics of end-milled surface textures are investigated for the purpose of tool wear monitoring. To analyze the anisotropic nature of end-milled surface textures, fractal analysis is applied on the image profiles along different directions as well as to the entire image. A 13-element feature vector made up of the extracted fractal features forms the multidimensional observation sequence that is used to train the HMM model. The HMM is successfully used to determine four distinct states of tool condition. This work shows that it is feasible to develop a tool wear monitoring system for end milling operations based on fractal analysis and HMM techniques.

References

1. Byrne, G., Dornfeld, D., Inasaki, I., Ketteler, G., König, W., Teti,R.: Tool condition monitoring (TCM) – the status of research and industrial application. Ann. CIRP **44/2**, 541–568 (1995)
2. Mannan, M.A., Kassim, A.A., Jing, M.: Application of image and sound analysis techniques to monitor the condition of cutting tools. Pattern Recogn. Lett. **21**, 969–979 (2000)
3. Whitehouse, D.J.: Typology of manufactured surfaces. Ann. CIRP **18**, 417–420 (1971)
4. Kassim, A.A., Mannan, M.A., Jing, M.: Machine tool condition monitoring using workpiece surface texture analysis. Mach. Vis. Appl. **11**, 257–263 (2000)
5. Turner, M.J., Blackledge, J.M., Andrews, P.R.: Fractal Geometry in Digital Imaging. Academic, Newyork (1998)
6. Chaudhuri, B.B., Sarkar, N.: Texture Segmentation using Fractal Dimension. IEEE Trans Pattern Anal. Mach. Intell. **17**(1), 72–77 (1995)
7. Sun Jing'ao, S., Anni, C.: Fractal based texture analysis for retrieval image data. In: APCC/OECC '99, Joint Conference of 5th Asia-Pacific Conference on Communications (APCC) and 4th Opto-Electronics and Communications Conference (OECC), vol. 2, pp. 845–848 (1999)
8. Russ, J.C.: Fractal Surfaces. Plenum, New York (1994)
9. Li, C.-G., Dong, S., Zhang, G.X.: Evaluation of the anisotropy of machined 3D surface topography. Wear **237**, 211–216 (2000)
10. Thomas, T.R., Rosén, B.-G., Amini, N.: Fractal characterisation of the anisotropy of rough surfaces. Wear **232**, 41–52 (1999)
11. Rabiner, L.R.: A tutorial on hidden Markov models and selected applications in speech recognition. Proc. IEEE **77**, 257–286 (1989)
12. Heck, L.P., McClellan, J.H.: Mechanical System monitoring using hidden markov models. Acoust., Speech Signal Process., IEEE Int. Conf., **3**, 1697–1700 (1991)
13. Atlas, L., Ostendorf, M., Bernard, G.D.: Hidden Markov models for monitoring machining tool-wear. Acoust. Speech Signal Process. IEEE Int. Conf. **6**, 3887–3890 (2000)